

Conductance-Voltage Relations in Large-Conductance Chloride Channels in Proliferating L6 Myoblasts

O. HURŇÁK and J. ZACHAR

*Institute of Molecular Physiology and Genetics, Slovak Academy of Sciences,
Vlárska 5, 833 34 Bratislava, Slovak Republic*

Abstract. Large-conductance chloride channels (maxi-Cl channels) were studied in cultured myoblasts (L6 rat muscle cell line); in excised (inside-out) and in cell attached membrane patches using a conventional patch clamp method.

The incidence of maxi-Cl channels was substantially higher in proliferating myoblasts, then in quiescent (bottom-attached) myoblasts (90% and 50% percent of examined cells, respectively). The maxi-Cl channels in myoblasts were present both in cell attached and excised patches.

The channel conductance at symmetric $[Cl] = 150$ mmol/l was 359 ± 42 pS ($n = 74$) in quiescent cells and 439 ± 10 pS ($n = 6$) in proliferating myoblasts respectively.

The conductance of the channel in quiescent cells increased with chloride concentration in symmetric NaCl rich solutions according to Michaelis-Menten curve with the saturation limiting conductance of about 640 pS (g_{max}) and $K_m = 112$ mmol/l.

The shift of the reversal potential upon increasing the pipette concentration of NaCl from 150 to 250 mmol/l was consistent with $P_{Na}/P_{Cl} = 0.1$. Neither the conductance nor the activation of the channel were dependent on the presence of calcium ions.

The bell-shaped steady state channel conductance-voltage relationship is asymmetric and can be fitted by two Boltzmann equations with different V_h and k constants; -25.6 mV and -6.8 mV, respectively, for the negative side and $+49.6$ mV and $+13.7$ mV for the positive side in quiescent cells. The corresponding values in proliferating myoblasts were as follows: -15.5 mV and -2.4 mV, respectively, for the negative side and $+31.4$ mV and $+6.8$ mV for the positive side. From the maximum slopes of the P_{open} versus V curves an estimate was made of the charges for the gates that close at negative (3.5) or positive (1.7) potentials, respectively, in quiescent cells. The corresponding values in myoblasts were 10.6 and 3.7, respectively.

The probability of one gate to be open was dependent on the state of activation

of the opposite gate as determined by prepulses of the opposite polarity.

The channel showed multiple (up to six) conductance levels that may develop in a step-like manner.

The onset of the full-grown maxi-Cl channel is fairly abrupt; it might, however, be preceded by a small conductance unit activity.

It is supposed that the differences between the quiescent myoblasts and proliferating myoballs might reflect increased expression of maxi-Cl channels in myoballs to perform as yet unknown role in the cell cycle and/or proliferation of the myoblasts.

Key words: Chloride channel — Large-conductance channel — Anion channel — Muscle cell line — Open probability — Rate of relaxation — Gating — L6 myoblasts — Myoballs — Voltage dependent channels — Patch clamp

Introduction

Since their discovery in primary cultures of skeletal muscle (myotubes) by Blatz and Magleby (1983) the high conductance chloride channels were found in all three types of muscle cells (skeletal, smooth and cardiac), in excitable and non-excitable neuronal cells, in several kinds of epithelial and endothelial cells and in blood cells, mostly lymphocytes (for a review see Hurňák and Zachar 1992). The functional significance of these channels remains unknown. We have described recently the existence of maxi-Cl channels at very early stages of undifferentiated myoblasts of the L6 rat muscle cell line (Hurňák and Zachar 1992), i.e. at a stage, where they form a prominent part of a rather poor channel mosaics. We therefore hypothesized that they might play a role in some basic functions of the cell, such as the volume regulation and/or the cell differentiation (see also Blatz and Magleby 1983). At least two conditions appear crucial for the progress in elucidation of their role in the cell functions: First, a correlated insight into their activation with supposed activities of the cell and second, a disclosure of modulation of their behaviour with physiological agents. In the following two papers we are characterizing further the conductance properties of the maxi-Cl channels in L6 myoblasts and bring new evidence concerning the increase of maxi-Cl channels in proliferating myoballs as compared with quiescent (bottom-attached) cells, and on differences in their properties as described in this paper and by specific blockators reported in the following paper (Zachar and Hurňák 1994).

Materials and Methods

Cells. The rat muscle cell line L6 (Yaffe 1968) was used in patch clamp experiments. The cell line was purchased from the American Type Culture Collection (A.T.C.C.; Rockville,

MD, USA). Cells for experiments were subcultured (maximum 6×) at regular time intervals to prevent fusion. Cells were seeded in plastic or glass dishes at required densities, usually at $2 - 5 \times 10^5$ cells/Petri dish in Dulbecco's modified Eagle's medium containing 20% fetal bovine serum and antibiotics: streptomycin, kanamycin, (100 µg/ml each) and penicillin (100 units), and were kept in a humidified atmosphere under 5% CO₂ / 95% O₂ at 37 °C. L6 myoblasts were taken for experiments 24–96 hr after plating. Before the experiment proper, the culture medium was exchanged for normal Krebs solution.

Electrophysiology. Currents were recorded in cell attached or excised (inside-out) configuration of the patch-clamp technique (Hamill et al. 1981) as described in detail elsewhere (Hurňák and Zachar 1992). Briefly, all recordings were made with an Axopatch 1C patch-clamp amplifier and CV-4 0.1/100 headstage (Axon Instruments, Foster City, CA, USA). Currents were low-pass filtered (1–2 kHz) by an eight pole Bessel filter. Data were acquired and analysed using an IBM AT compatible computer with an analog-to-digital interface board (Labmaster DMA, Scientific Solutions Inc., Solon, OH, USA) using pClamp 5.5.1 software (Axon Instruments). The ramp-pulse recordings were evaluated using a software developed in our own laboratory (Stavrovský et al. 1992). Evaluation of ramp protocols, non-linear fitting of data and determination of voltage-dependence of channel activation was described elsewhere (Hurňák and Zachar 1993). In all figures potentials represent pipette potentials.

Solutions. The standard bath contained a NaCl saline consisting of (mmol/l): 150 NaCl; 0.5 CaCl₂; 20 HEPES; pH 7.4 or a Krebs solution (mmol/l): 135 NaCl; 5 KCl; 1 CaCl₂; 2 MgCl₂; 20 HEPES; 5 glucose; pH 7.4 at 23 °C. In most experiments the pipette solution was the same as that in the bath solution. The bath solutions used for testing the $g_{Cl} - [Cl]_o$ relation and the selectivity, respectively, contained 150 mmol/l NaX, where X has the test or replacing anion. Low Cl⁻ solutions were made by equimolar replacement with gluconate or methanesulphonate. High Cl⁻ solutions were hypertonic NaCl solutions. All experiments in the inside-out patch configuration that required exchange of solutions were performed with the tip of the patch pipette positioned inside a perfusion capillary with a diameter of about 1 mm. The reference Ag-AgCl pellet electrode was connected to the bath by means of 3 mol/l KCl bridge. The junction potentials as measured against this electrode were corrected where appropriate (Neher 1992).

Where appropriate, data are cited as means ± S.E.M.

Results

Basic characteristics of single channel currents in inside-out excised patches from quiescent L6 myoblasts are demonstrated in Fig. 1A showing ten consecutive responses to voltage steps of 10 mV (4.2 s in duration) from the holding potential of 0 mV in both the positive and negative directions. Both the pipette and the bath solutions were of the same composition (150 mol/l NaCl, 0.5 mmol/l CaCl₂). The channel was open most of the time at small membrane displacements (±10 mV, ±30 mV), but inactivated quickly at larger voltage steps. Transitions between closed and open states were abrupt in response to negative displacements in contrast to multiple steps (see arrows) observed in response to positive membrane potential displacements (see below the section on subconductance states.) Fig. 1B

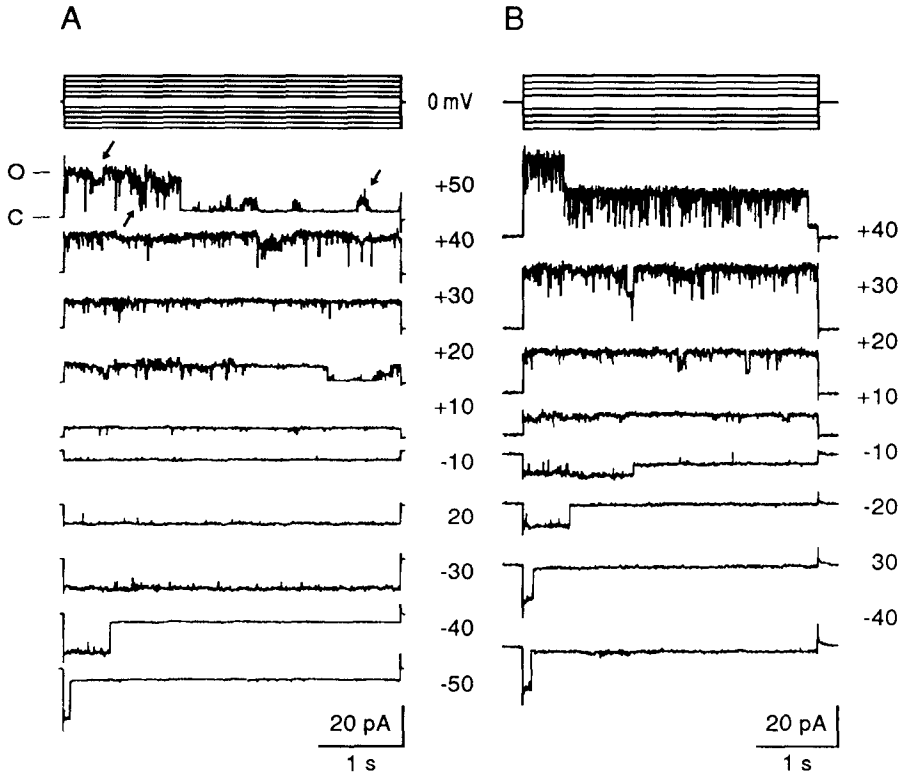


Figure 1. Single channel current records from excised patches (inside-out) of a quiescent (bottom-attached) myoblast (*A*) and a proliferating rounded myoball (*B*). Successive records to command pulses from +50 to -50 mV (*A*) or +40 to -40 mV (*B*) respectively in 10 mV steps from a holding potential of 0 mV. Duration of test pulses 4200 ms in (*A*) and 3600 ms in (*B*); interpulse interval 10 s; sampling interval 2 ms. *O* - closed state; *C* - open state of an activated channel. The subconductance states are marked by arrows (pulse to +50 and +20 mV). Note extensive flickering in substates. Symmetrical (patch pipette // bath) solutions (mM/l): *A* - 150 NaCl, 0.5 CaCl₂; *B* - Krebs solution.

shows records of unit channel activity in excised inside-out patches from rounded proliferating myoblasts (myoballs) obtained under similar experimental conditions (Krebs solution with $[Cl^-] = 147$ mM/l; voltage step duration 3.6 s). The maxi Cl⁻ channels in myoballs were present both in cell-attached and excised patches. The recordings showed similar patterns as those from the quiescent myoblasts including the asymmetry to pulses of opposite polarity.

Channel conductance

The channel conductance corresponding to the main open level was determined

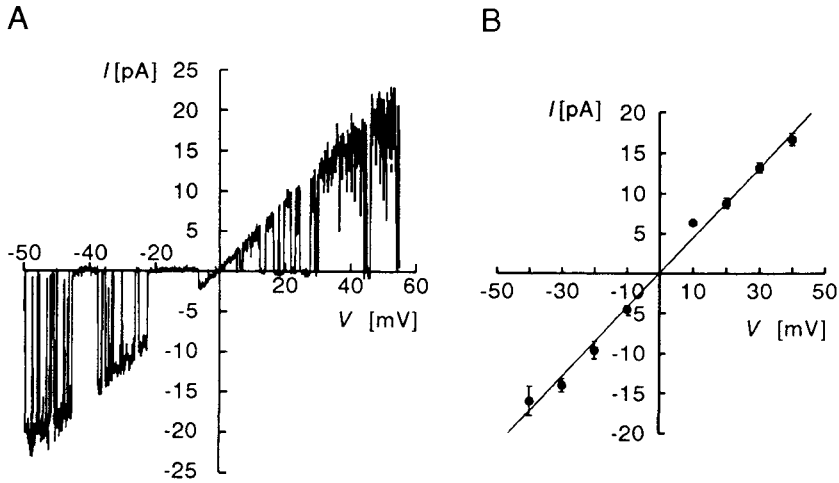


Figure 2. Current-voltage relations in quiescent myoblasts and proliferating myoballs. *A.* Single-channel currents in quiescent myoblasts to a symmetrical voltage ramp pulse from -60 to $+60$ mV applied within 1 s. The leakage membrane conductance slope was subtracted (see text). Slope of the best fit line through the open channel levels then gives directly the channel conductance, $g = 395$ pS. Symmetrical solutions ($[Cl] = 150$ mmol/l). *B.* $I - V$ relation in a proliferating myoball determined from the records like those demonstrated in Fig. 1. The channel conductance, $g = 439$ pS.

from the records like those demonstrated in Fig. 1 or directly obtained from current-voltage ramp records (Fig. 2A) using the procedure of Stavrovský et al. (1992). The straight line that can be fitted through the open channel levels in Fig. 2A (quiescent cell) represents the $I - V$ plot and has a slope of 395 pS. The average value of conductance in symmetrical 150 mmol/l NaCl was 359 ± 42 pS ($n = 74$). The line crosses the ordinate close to 0 mV. In the solution used this value would be expected for the equilibrium potential of a Na^+ , Cl^- , or a nonselective channel. The shift of the reversal potential upon increasing the pipette concentration of NaCl to 250 mmol/l was consistent with $P_{Na}/P_{Cl} = 0.1$ indicating the chloride nature of the high-conductance channel. The channel conductance was not influenced by variation of the Ca^{2+} ions in either internal or external surroundings of the membrane. The average current-voltage relation in myoballs in symmetrical Krebs solution ($[Cl] = 147$ mmol/l) is demonstrated in Fig. 2B. The conductance, $g_{Cl} = 439 \pm 10$ pS ($n = 6$) is higher than in quiescent cells under comparable experimental conditions.

The chloride conductance in the main state, g_{Cl} was a function of the Cl concentration, $[Cl]_i$ on the intracellular side of the membrane. Fig. 3 shows the $[Cl]_i$ versus g_{Cl} plot obtained with the 150 mmol/l NaCl in the pipette and changing the

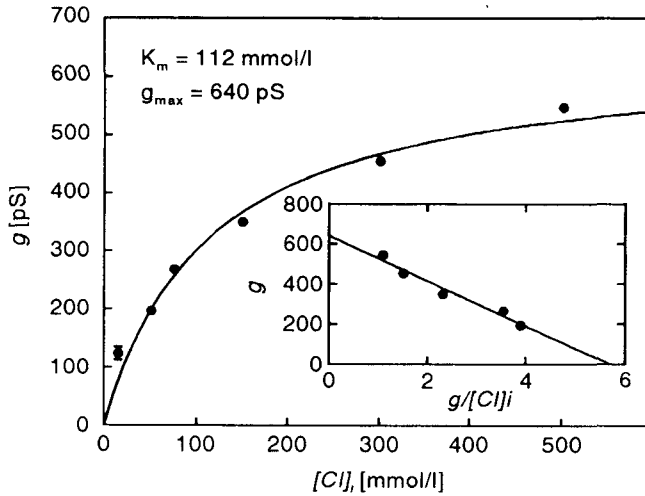


Figure 3. Nonlinear chloride activity (*abscissa*) – conductance (*ordinate*) relation of high-conductance channels in membrane patches excised from quiescent L6 myoblasts. The best fit line through the experimental points represents Michaelis-Menton curve drawn from Equation (1) in the text. *Inset:* linearized (Eadie-Hofstee) plot of the relation. $g_{\max} = 640$ pS; $K_m = 112$ mmol/l. Symmetrical NaCl solutions. Each point represents a mean \pm S.E.M. of at least 3 measurements in different patches except for $[Cl] = 500$ mmol/l (two measurements).

chloride concentration on the intracellular side of the patch membrane. In solutions with $[Cl]_i < 150$ mmol/l, NaCl was replaced by Na methanesulphonate or Na gluconate (25 mmol/l, $n = 3$; 50 mmol/l, $n = 5$). Solutions with $[Cl]_i > 150$ mmol/l were hypertonic NaCl solutions (300 mmol/l, $n = 5$; 500 mmol/l, $n = 2$). The curve through experimental points was fitted by the Michaelis-Menten equation:

$$g_{Cl} = g_{\max} / (1 + K_m / [Cl]_i), \quad (1)$$

where K_m is the concentration for half-maximal conductance, g_{\max} is saturating conductance and $[Cl]_i$ is concentration of Cl^- ions. The inset shows linearized (Eadie-Hofstee) plot of the relation for evaluation of $g_{\max} = 640$ pS and $K_m = 112$ mmol/l, respectively. It follows from Fig. 3 that the ionic fluxes through the high-conductance anion channel saturate as ionic concentrations are raised well above their physiological levels. This is a clear indication that the permeation of Cl^- ions through the channel deviates from the independence principle (Hille 1992).

Incidence of channels

The maxi-Cl channels in bottom attached L6 myoblasts were quiescent for a varying period between few seconds and several tens of minutes before they become

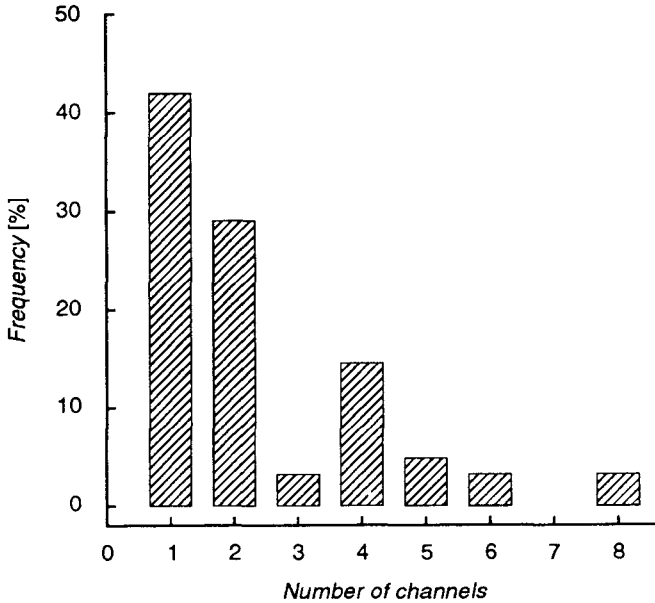


Figure 4. Frequency distribution of the numbers of channels observed in membrane patches from L6 myoblasts.

activated as already documented elsewhere (Hurňák and Zachar 1992). During the chosen waiting interval of 30 min the channels were observed in 69 out of 138 excised patches. The number of channels in a patch varied a great deal as shown in Fig. 4; and shows a Poisson frequency distribution. The incidence of maxi-Cl channels per patch in proliferating myoblasts was much higher almost in every cell examined (32/38). The channels appeared already in cell attached patches and continued to be active after excision of the patch membrane from the cell. The number of channels in the membrane varied a great deal, comparably to the variation in quiescent cells.

The onset of the channel activity is an abrupt event. In a small proportion of cell attached patches we observed, however, a small amplitude unit channel activity, which preceded the onset of full amplitude maxi-Cl channel events. Fig. 5A shows a long record (≈ 20 s) of such a single channel current activity at the +80 mV holding potential. Fig. 5B shows a corresponding current-voltage relation with a slope $g = 18$ pS determined from the records such as that shown in Fig. 1B at four other voltage steps. The current reversed at a potential close to 0 mV and the relation showed no rectification. During the measurement the channel activity passed into a full-grown maxi-Cl channel activity with typical large amplitude single channel currents and inactivation at higher membrane potential displacements.

A



B

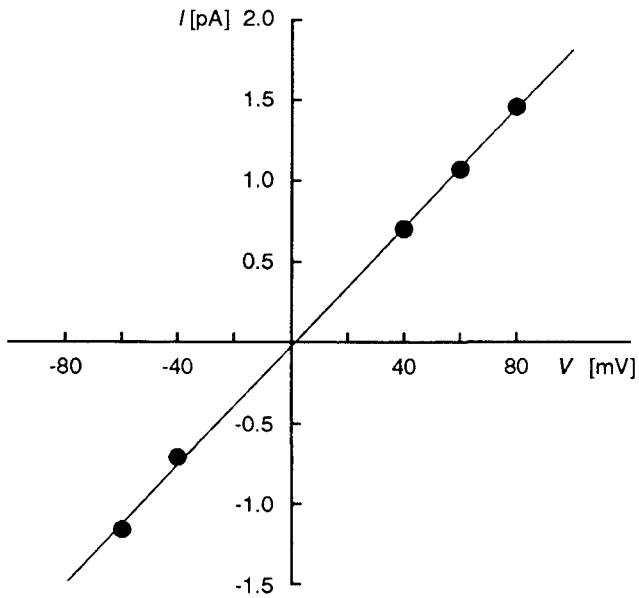


Figure 5. Small conductance unit channel currents preceding the appearance of full-grown maxi-Cl channel activity. *A*: Continuous record of unit channel activity just prior to onset of large-conductance unit channel currents. Holding potential +80 mV. *B*: Current-voltage relation with a slope, $g = 18$ pS.

We never observed the small conductance channel activity to reappear at higher membrane voltage steps (e.g. 80 mV), when the maxi-Cl channel activity is absent and when the small conductance channel activity is expected to be present (Fig. 1A). The coincidence of both events occurs in such a casual relation that it precludes independent events.

Voltage dependence

The high-conductance chloride channel spent most of its time in the open state in the voltage range close to the holding potential (about ± 15 mV). The probability of the channel to be in the open state, however, steeply decreased by larger displacements of the membrane potential from the holding potential (0 mV) as already shown in Fig. 1. Fig. 6A demonstrates the voltage dependence (V) of the steady state probability of the channel being in the open state (P_{open}) in quiescent cells. The P_{open} versus V plot was constructed from the proportion of time the channel spent in the open state in relation to the total time of recording the channel activity to a voltage step. The probability plot is clearly asymmetrical. The probability of the channel to remain in the open state was clearly higher at positive membrane

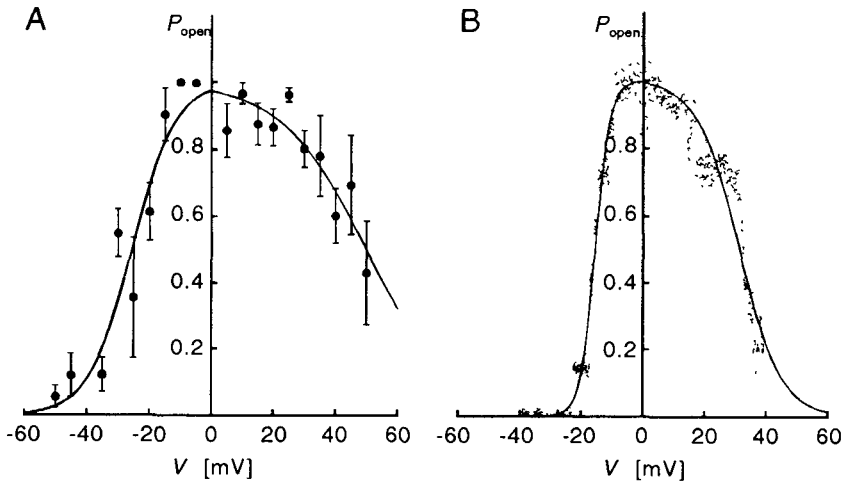


Figure 6. Voltage dependence (V) of the steady-state probability (P_{open}) of the channel being in the open state. The bell-shaped relations were determined from the records like those demonstrated in Fig. 1. *A* (quiescent cells): The curve was fitted as the sum of two Boltzmann equations (given in the text) with coefficients $V_h = -25.6$ mV and $k = -6.8$, respectively, for the negative side and $+49.6$ mV and $+13.7$ for the right side. *B* (myoballs): The curve was fitted as the sum of two Boltzmann equations with coefficients $V_h = -15.5$ mV and $k = -2.4$, respectively, for the negative side and $+31.4$ mV and $+6.8$ for the right side. Note asymmetric shape of dependence of P_{open} on negative and positive voltage pulses (V), respectively.

potential displacements than in the opposite direction.

The bell-shaped dependence of open probability (P_{open}) on voltage (V) was described by two Boltzmann equations of the form:

$$P_{\text{open}} = P_{\text{max}} / \{1 + \exp[(V - V_h)/k]\}, \quad (2)$$

where P_{open} is the steady-state probability of the channel being in the open state, V_h is the voltage at $P_{\text{open}} = 0.5$ and k is the slope factor and represents the voltage sensitivity of activation. The fitted values of V_h and k were -25.6 mV and -6.8 , respectively, for the negative side and $+49.6$ mV and $+13.7$ for the positive side.

From the maximum slopes of the P_{open} versus V curve an estimate can be made of the charges for the gates that close at negative or positive potentials, respectively (Almers 1978, Hille 1992). The charges calculated were 3.5 for the negative and 1.7 for the positive side, respectively.

Similar behaviour was observed also in proliferating myoballs (Fig. 6B). The fitted values of V_h and k were -15.5 mV and -2.4 respectively, for the negative side and $+31.4$ mV and $+6.8$ for the positive side. Mean values are given in Table 1. It is evident that the steepness of the relation is greater in myoballs in comparison with quiescent cells.

The charges (z) calculated from the bell shaped relations (Table 1) were higher in myoballs in comparison with the myoblasts.

Table 1. Boltzmann's parameters and gating charges

Cell	$V_{h(n)}$	$k_{(n)}$	z	$V_{h(p)}$	$k_{(p)}$	z	Ref
L6 (quiescent)	-25.6	-6.8	3.5	49.6	13.7	1.7	1
L6 (myoballs)	-15.5	-2.4	10.6	31.4	6.8	3.7	1
BC3H1 myoblasts	-53.0	-8.4	3.0	41.0	10.2	2.5	2
T lymphocytes (e.p.)	-22.8	-4.4	5.7	18.0	2.6	9.6	3
T lymphocytes (c.a.)	-	-	-	-55.8	13.1	3.2	4
Epithelial (bile duct)	-	-	≈ 2.4	-	-	≈ 2.4	5§
Epithelial (fetal)	-41.9	-0.7	36.2	-	-	-	6*
Neuroblastoma	-20.3	-6.3	4.0	36.0	10.0	-	7*
Skeletal muscle	-41.3	-	4.3	288.0	61.0	-	8
Skeletal muscle [Ca]	-19.5	-4.9	5.2	59.8	13.0	1.9	8*

Notes: V_h is the midpoint potential; k is the slope factor; (n) and (p) signs denote parameters of the negative and positive side of the bell-shaped plot, respectively; * approximate values calculated from the published $P_{\text{open}} - V$ curves; § - calculated from the e -fold change ≈ 10 mV; e.p. - excised patch; c.a. - cell-attached patch; [Ca] - the effect of high Ca concentration

Ref.: 1 Hurňák and Zachar (this paper); 2 Hurňák and Zachar 1993; 3 Schlichter et al. 1990; 4 Pahapill and Schlichter (1992); 5 McGill et al. 1992; 6 Kemp et al. 1993; 7 Bettendorff et al. 1993; 8 Woll and Neumcke 1987

The probability plot is matched on the macroscopic level by relaxations of the ensemble average currents at appropriate voltage steps as demonstrated in Fig. 7A (quiescent cells) and Fig. 7B (myoballs). The mean currents show different rates of relaxation depending on the polarity of the voltage jump. The relaxation can be fitted by a single exponential according to the equation:

$$i = a \exp(-t/\tau) + c \quad (3)$$

where i is current, t is time, τ is time constant of relaxation, a is current at $t = 0$ and c is leak current.

The relaxation was significantly slower in ensemble currents evoked by positive voltage displacements in the demonstrated examples. The sidedness, however, varied a great deal in different cells. The values of τ (in the quiescent cell) were 1910, 625 and 236 ms at negative, and 29900, 13500 and 971 ms at positive voltage steps (± 20 , ± 40 , ± 60 mV) respectively. The values of τ in myoballs were lower (3648 ms at 20 mV and 53 ms at -20 mV in Fig. 7B) in accord with the P_{open} versus V relationship (Fig. 6).

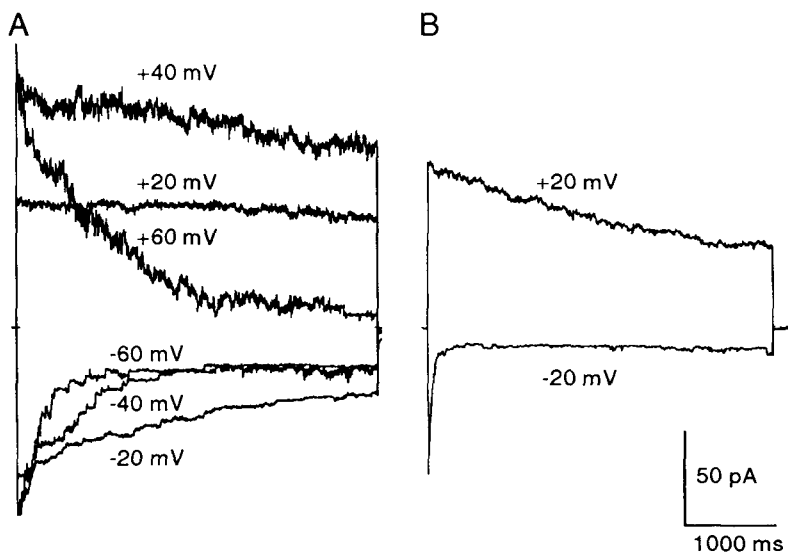


Figure 7. Ensemble averages of single-channel currents in excised patch at different potential steps in quiescent cells (A) and proliferating myoballs, respectively (B). Note asymmetry of responses to symmetrical voltage steps of opposite polarity from the holding potential of 0 mV. Five averaged current traces at every step. The repetition interval was 15 s, the sampling interval 5 ms and the pulse duration 4750 ms. Symmetrical Cl solutions. A: 150 mmol/l Cl⁻; B: Krebs solution.

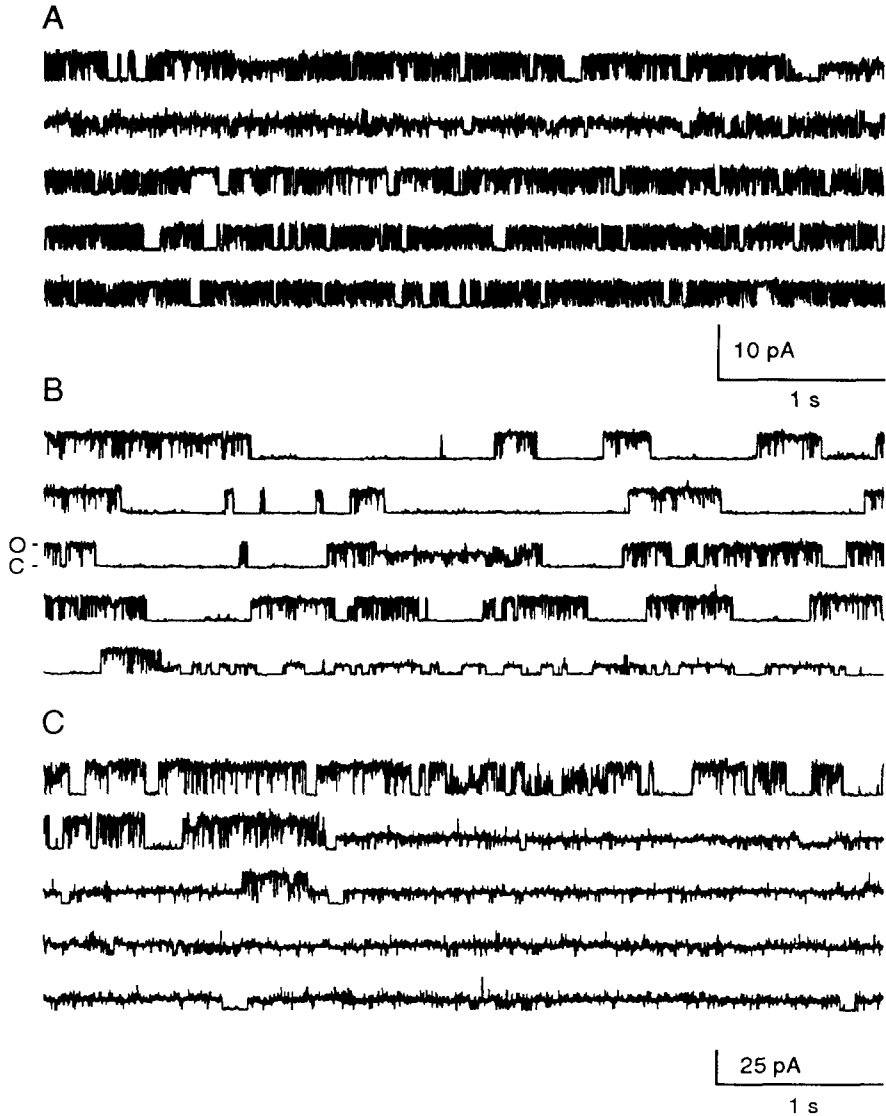
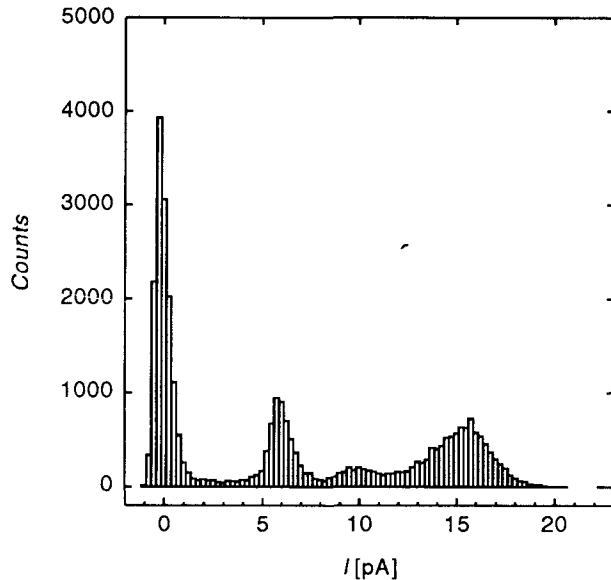


Figure 8. Segments of continuous records (25.6 s each) of unit current activity of the high-conductance channel at three membrane potentials (quiescent cells): A +10 mV, B +40 mV, C +50 mV. Channel openings are upward with outward currents (inward movement of Cl^- ions); c—closed state; o—open state. Note several substates, preferences to be in a substate, flickerings from substates, and bursting character of channel activity. Channel may rest in a substate level for several seconds. Pipette and bath both contained 150 mmol/l NaCl (0.5 mmol/l CaCl_2).

Subconductance states

As already mentioned at the beginning of this section (Fig. 1), the high conductance channel showed multiple substate levels that formed a characteristic feature of the channel behaviour at positive membrane displacements. Fig. 8 shows long duration single channel current recordings (≈ 30 s) from an excised inside-out membrane patch at three membrane depolarizations (channel openings are upward, and currents are outward). The channel was open most of the time at +10 mV (Fig. 8A) and displayed frequent transitions between the open amplitude level and the base line. After about 5 s from the start (second row) the channel spent about 4 s in a subconductance state with frequent flickerings to the closed level. At +40 mV displacement of the membrane potential (Fig. 8B) the channel conductance fluctuated in long (≈ 1 s) bursts between the open and the closed level. After about 5 s (fifth row) the conductance started to fluctuate between a subconductance level and the closed state. At +50 mV (Fig. 8C) the channel conductance fell to this subconductance level after about 6 s from the start of recording with rare transitions to a closed level, but frequent flickerings in both upward and downward directions.

Figure 9. Amplitude histogram constructed from continuous recordings (1 min) of single channel currents at a membrane displacement of +20 mV from the holding potential of 0 mV. The same membrane patch as in Fig. 8. At least two substate levels in addition to the full level can be recognized.



When the records like those in Fig. 8 were analysed for subconductance states, the most frequent substate level (Fig. 9) corresponded to about one third of the main conductance level (the full open state). The histogram shows also clearly a sublevel at about 2/3 of the full open level.

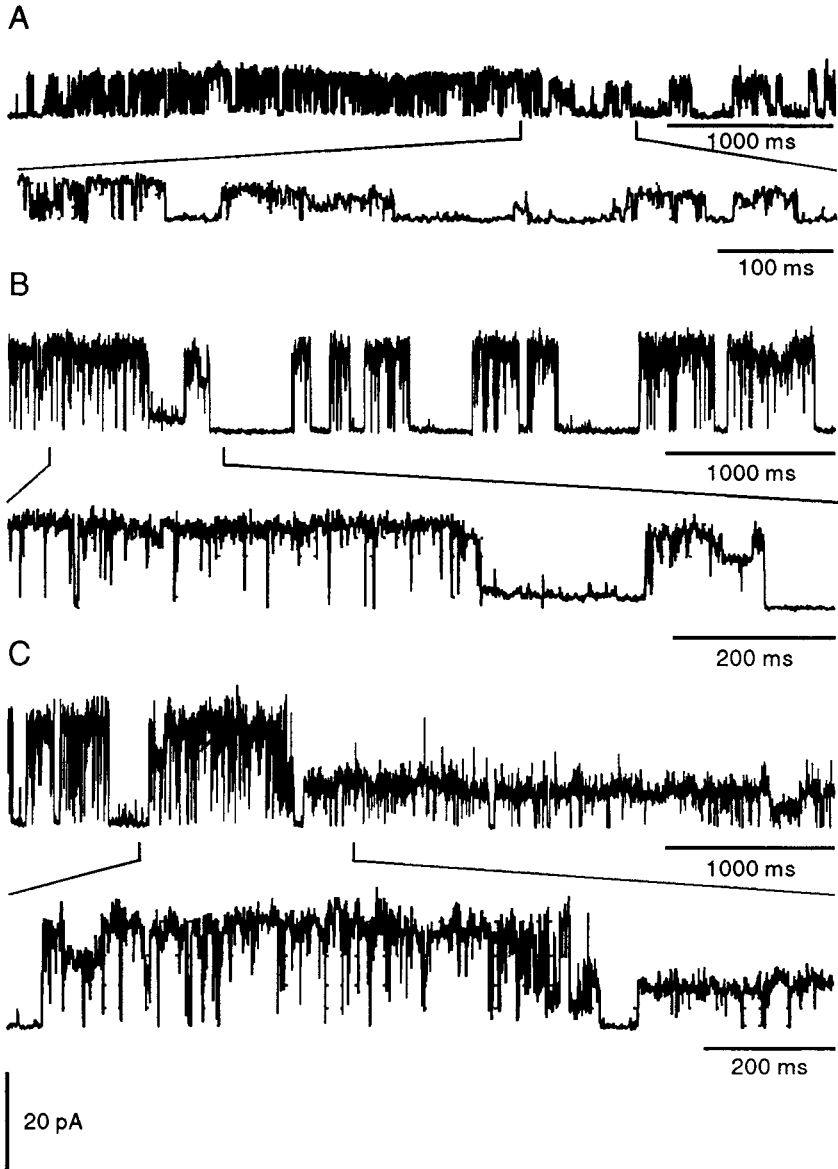


Figure 10. Segments of long continuous single channel records from an excised patch with typical substates episodes. Membrane potential was displaced from holding potential of 0 mV for the whole period of recording (1 min) to +20 mV (A), +40 mV (B), +50 mV (C). Expanded parts of the record are shown below each trace. Subconductance levels are indicated by dotted lines.

By closer inspection of the records further sublevels can be encountered as well. Fig. 10 shows three expanded segments from the series of long records shown in Fig. 8. A number of new subconductance levels (in addition to those detected from histograms) can be easily recognized; e.g. the preferred final level in Fig. 8C can be easily subdivided into two sublevels (Fig. 10C). New sublevels were present also at two other depolarizations (+20 mV, Fig. 10A; +40 mV, Fig. 10B respectively). It follows that up to six distinct sublevels can be recognized in the records of maxi-Cl channel activity in L6 myoblasts with an amplitude of ≈ 60 pS at $[Cl] = 150$ mmol/l.

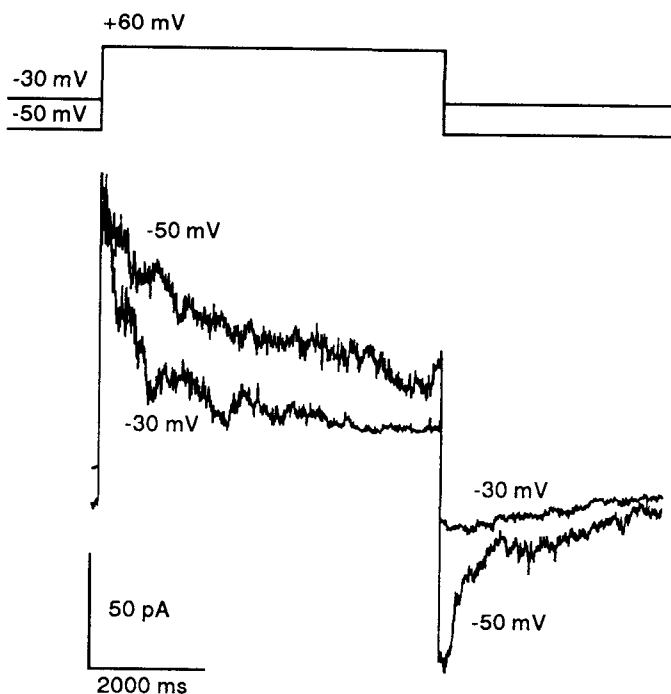


Figure 11. The effect of holding potential on the rate of channel relaxation. Ensemble average currents from six consecutive unit channel responses to +60 mV. Holding potential: -50 mV and -30 mV, respectively.

Voltage dependence of channel activation

Fig. 11 demonstrates the effect of holding potential (HP) on the rate of relaxation of ensemble average currents to voltage steps of +60 mV. When the membrane potential difference was increased from -30 to -50 mV, the rate of relaxation

decreased three times, from 1.6 s^{-1} ($\tau = 625 \text{ ms}$) to 0.45 s^{-1} ($\tau = 2203 \text{ ms}$) in response to $+60 \text{ mV}$ voltage step. The effect was quite the opposite after the end of the test pulse; an increase of the rate of deactivation from 0.14 s^{-1} (at $HP = -30 \text{ mV}$) to 1.46 s^{-1} (at $HP = -50 \text{ mV}$) was observed.

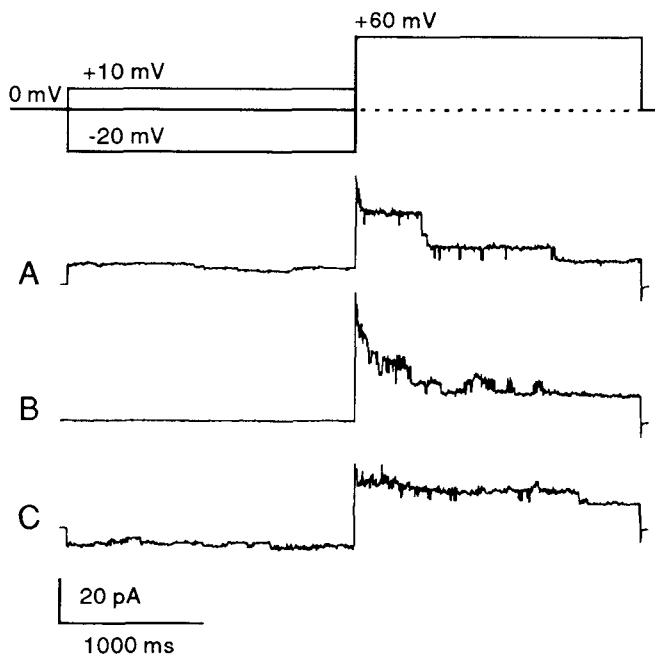


Figure 12. The effect of conditioning prepulses on the channel activity. Ensemble average currents from six consecutive unit channel responses to $+60 \text{ mV}$ pulses. Holding potential was 0 mV . (A) conditioning pulse from 0 to $+10 \text{ mV}$; (B) control record; (C) conditioning pulse from 0 to -20 mV .

A similar effect can be demonstrated by means of conditioning pulses as shown in Fig. 12. A conditioning prepulse to -20 mV slowed down appreciably the time constant of relaxation (Fig. 12C) as compared with the ensemble average current in response to $+60 \text{ mV}$ voltage step from the holding potential, $HP = 0 \text{ mV}$ (Fig. 12B); i.e. from 257 ms to 2512 ms , respectively. The effect of the prepulse of the same polarity ($+10 \text{ mV}$) was less pronounced as follows from the record in Fig. 12A; the number of six summated responses was not sufficient to obtain a curve smooth enough for determination of τ ($\approx 600 \text{ ms}$).

Discussion

The main difference between the quiescent myoblasts, i.e. those attached to the bottom of the culture dish, and the proliferating myoballs concerns the higher probability of incidence of maxi-Cl channels in patch clamp trials in rounded-up cells. It should also be noted that the maxi-Cl channels were present in myoballs in cell-attached patches as well, contrary to the opposite claims in literature on large conductance Cl channels. The higher incidence of maxi-Cl channels could mean that the density of channels in the membrane of proliferating myoballs increased in comparison with quiescent cells. The physiological significance of this fact might be looked for in a role of the high-conductance Cl channels in the cell cycle and/or proliferation of the myoblasts. The proliferation was not synchronized in these experiments; the exact phase of the cell cycle of the observed cells is therefore difficult to ascertain. The membrane potential of the rounded myoballs was very low; this might indicate that the cells were mostly in the interphase, perhaps in the early G₁ phase; if we suppose that the changes in membrane potential during the cell cycle are similar to those cells, where the membrane potential was actually measured (Sachs et al. 1974). The membrane potential begins to rise, as follows from the above work, about the time that DNA synthesis begins. It remains to be elucidated whether the increased expression of maxi-Cl channels in rounded-up cells are causally related to the mitotic activity or represent only secondary events to the cell cycle metabolic changes.

It is interesting to note in this connection the results of Takahashi et al. (1993). They found profound changes in Ca²⁺ dependent K⁺ current during the cell cycle in HeLa cells, i.e. an increase of the K⁺ current in the early G₁ phase and a decrease of the K⁺ current in the S phase of the cell cycle. The number and density of K⁺ channels changed accordingly to changes in the K⁺ current. How are these changes in the number of channels related to the cell cycle and/or proliferation, remains, however, to be shown.

Another difference between the quiescent cells and myoballs concerns the probability of the channel being in the open state in dependence on the applied negative and positive voltage step, respectively (Fig. 6). The bell shaped $P_{\text{open}} - V$ relationship is asymmetric in both quiescent myoblasts and myoballs, respectively; the dependence on the voltage (V) is, however, substantially steeper in myoballs in comparison with quiescent myoblasts. Since substantially lower values of the Boltzmann parameters were found in T lymphocytes (Table 1) in cell excised patches (Schlichter et al. 1990) in comparison with cell attached patches (Pahapill and Schlichter 1992), the difference might be related to the internal side of the channel being in contact with the cell interior in cell-attached patches in T lymphocytes. As follows from the experiments (amphibian skeletal muscle) of Woll and Neumcke (1987), the steepness of the negative branch of the $V - P_{\text{open}}$ curve shows a clear

dependence on the ionic composition of the solutions. They found that the mid-point potential $V_{h(n)}$ was shifted to more positive potentials in high [Ca] solutions and to more negative potentials in high pH solutions. This fact could be however hardly responsible for the observed differences, as they were encountered in similar [Cl] solutions. It might then be supposed that the discussed differences between the channel $P_{open} - V$ parameters in excised patches of quiescent and proliferating myoblasts are genuine and have to be perhaps searched for in differences of channel substructure. As follows from Table 1, very steep decay of maxi-Cl channel inactivation was described by Kemp et al. (1993) in fetal alveolar epithelial cells which were open at large positive potentials and closed quickly in response to negative membrane potential displacements greater than about 40 mV. It remains to be demonstrated, whether the asymmetric channel behaviour in the $V - P_{open}$ relationship represents a characteristic of the newly formed channels or channels during the development.

The third difference concerns the value of the channel conductance which was some 70 pS higher in myoballs in symmetrical [Cl] (≈ 150 mol/l). The cause of this difference remains unknown. As a first step in trying to resolve this puzzle, it will be, however, necessary to repeat the measurements in parallel (not successive) experiments on both the quiescent myoblasts and proliferating myoballs.

All other characteristics of high-conductance Cl channels in quiescent and rounded-up proliferating myoballs were fairly similar and their quantitative parameters fell within those encountered in other cell membranes.

It follows from Fig. 3 that the ionic fluxes through the high-conductance anion channel saturate as ionic concentrations are raised well above their physiological levels. This is a clear indication that the permeation of Cl^- ions through the channel deviates from the independence principle. A similar behaviour was observed in maxi-Cl channels in T lymphocytes (Schlichter et al. 1990) with $g_{max} = 581$ pS and $K_m = 120$ mmol/l under comparable experimental conditions.

The reversal potential measurements indicated that the P_{Na}/P_{Cl} was about 0.1, in agreement with data obtained in other chloride channels (e.g. Franciolini and Nonner 1987). Similar P_{Na}/P_{Cl} values (0.1–0.2) were already found in maxi-Cl channels by Gray et al. (1984) in cultured Schwann cells, by Nelson et al. (1984) in epithelial cells, and by Schwarze and Kolb (1984) in chicken myotubes. The nature of permeation in chloride channels might be thus imagined to be similar as suggested for anion channels by the latter authors: i.e. by means of activated complex in the selectivity region which includes an adsorbed cation to a negatively charged group and the permeating anion.

The channel conductance reaches the theoretical limits (Hille, 1992) of conductances calculated using Ohm's law and the diffusion equation. This is based on the assumption that the channel represents a uniform structure and not a cooperative ensemble of subunits which constitute the channel. The latter interpretation

could be assumed from the characteristics of subconductance states of the large-conductance chloride channels, which are a common property of these channels. Several substates (1–16) were demonstrated in this type of Cl channels (Gray et al. 1984; Geletyuk and Kazachenko 1985; Krouse et al. 1986; Bolotina et al. 1987; Woll et al. 1987; Schlichter et al. 1990; Becq et al. 1992; Groschner and Kukovetz 1992; Hurňák and Zachar 1992, 1993; McGill et al. 1992; Olesen and Bundgaard 1992; Kemp et al. 1993). Our finding of several conductance levels could be hardly ascribed to a single population of uncoordinated, stochastically active 60 pS channels. Such a model can be ruled out by the observed characteristics of the openings and the statistics of their occurrence (Läuger, 1985; Fox, 1987). First, if openings resulted from the random simultaneous super-position of two to six 60 pS channels, the frequency of appearance of the progressively larger conductances should approximate an inverse power series with extremely small chance of appearance of the maximum pS level. Second, random superposition would only rarely result in smooth transitions to a large conductance level, whereas we have routinely observed such transitions (Fig. 10). Substates could be expected from certain interpretations of ion channel models that visualize closure as resulting from a helical twisting (Catterall, 1988; Millhauser, 1990) or tilting (Unwin, 1989) of the pore-forming subunits. If we assume that in the open state, a polar region of an amphipathic transmembrane helix covers the wall of the aqueous pore, then the twisting motion of the subunits could move nonpolar groups into the channel, and thus occlude it. Bennett et al. (1991) have elaborated such a model for the connexon, which behaves in many respects – e.g. by $P_{\text{open}} - V$ relationship – like large-conductance Cl channels. It was even suggested that porins might form the biochemical basis of the large-conductance Cl channels (Babel et al. 1991; Thinnes 1992). If a similar model was applied to the functioning of the maxi-Cl channel, one had to postulate that the fully open ≈ 360 pS channel has each of its six subunits free to twist independently of the other five. The assumption of six subunits forming the basis of channel behaviour is, however, as yet difficult to reconcile with the varying number and values of subconductance levels as well as with values of small conductance unit channel activity (≈ 20 mV) which is thought to form a starting component of the full-grown maxi-Cl channel.

Small conductance unit channel currents which preceded the onset of a full-grown maxi-Cl channels were observed, however, only rarely. The main reason why we assume that they are causally related to the large-conductance Cl channels is the fact that they developed always into large conductance Cl channels. They are short-lived events; it was even difficult to obtain a current-voltage relation of these units because of their short life span. Second, we never observed their activity when the maxi-Cl channels were deactivated. In a recent paper Bettendorff et al. (1993) were able to activate these small conductance channel units preceding the onset of full-amplitude maxi-Cl channels by thiamine triphosphate, a novel activator of the maxi-Cl channels.

The bell-shaped steady state open channel probability – voltage relationship represents a common property of several classes of channels, e.g. gap junctional channels (Wang et al. 1992; Chen and DeHaan 1992), porins (Jap and Walian 1990; Benz et al. 1992) and/or VDAC channels (Thinnes 1992) and belongs with the high values of channel conductance to the essential characteristic features of the maxi-Cl channels (Woll and Neumcke 1987; Schlichter et al. 1990; Pahapill and Schlichter 1992; McGill et al. 1992; Groschner and Kukovetz 1992; Hurňák and Zachar 1993; Kemp et al. 1993; Bettendorff et al. 1993).

Two alternative models have been proposed (Harris et al. 1981) for the gating of the type represented by the bell-shaped type of $P_{\text{open}} - V$ behaviour, i.e. an independent gating model and a contingent model, respectively. The latter model assumes that the closed gate of the polarized channel has to open before the other gate in series can open. This view seems to be corroborated by the experiments with conditioning prepulses and/or variation of the holding potential (Figs. 11 and 12), which indicate that the gates are reciprocally related. This assumption is expected to be tested in further experiments.

Acknowledgements. This work was supported partly by a grant (2/999039/93 GAV) to J. Z. The authors wish to thank Dr. Daria Zacharová for valuable suggestions during the course of experiments and useful comments on the manuscript.

References

- Almers W. (1978): Gating currents and charge movements in excitable membranes. *Rev. Physiol. Biochem. Pharmacol.* **82**, 96–190
- Babel D., Walter G., Götz H., Thinnes F. P., Jürgens L., König U., Hilschmann N. (1991): Studies on human porin. VI. Production and characterization of eight monoclonal antibodies against the human VDAC “Porin 31HL” and their application for histopathological studies in human skeletal muscle. *Biol. Chem. Hoppe-Seyler* **372**, 1027–1034
- Becq F., Fanjul M., Mahieu I., Berger Z., Gola M., Hollande E. (1992): Anion channels in a human pancreatic cancer cell line (Capan-1) of ductal origin. *Pflugers Arch.* **420**, 46–53
- Bennet M. V. L., Barrio L. C., Bargiello T. A., Spray D. C., Hertzberg E., Saez J. C. (1991): Gap junctions: New tools, new answers, new questions, *Neuron* **6**, 305–320
- Benz R., Maier E., Thinnes F. P., Goetz H., Hilschmann N. (1992): Studies on human porins: VII. The channel properties of the human B-lymphocyte membrane-derived “Porin 31HL” are similar to those of mitochondrial porins. *Biol. Chem. Hoppe-Seyler* **373**, 295–303
- Bettendorff L., Kolb H.-A., Schoffeniels E. (1993): Thiamine triphosphate activates an anion channel of large unit conductance in neuroblastoma cells. *J. Membrane Biol.* **136**, 281–288
- Blatz A. L., Magleby K. L. (1983): Single voltage-dependent chloride selective channels of large conductance in cultured rat muscle. *Biophys.J.* **43**, 237–241

- Bolotina V., Borecký J., Vlachová V., Baudyšová M., Vyskočil F. (1987): Voltage-dependent Cl channels with several substates in excised patches from mouse neuroblastoma cells. *Neurosci. Lett.* **77**, 298—302
- Catterall W. A. (1988): Structure and function of voltage-sensitive ion channels. *Science* **242**, 50—61
- Chen Y., DeHaan R. L. (1992): Multiple-channel conductance states and voltage regulation of embryonic chick cardiac gap junctions, *J. Membrane Biol.* **127**, 95—111
- Fox J. A. (1987): Ion channel subconductance states. *J. Membrane Biol.* **97**, 1—8
- Franciolini F., Nonner W. (1987): Anion and cation permeability of a chloride channel in rat hippocampal neurons. *J. Gen. Physiol.* **90**, 453—478
- Geletyuk V. I., Kazachenko V. N. (1985): Single Cl-channels in molluscan neurones: multiplicity of the conductance states. *J. Membrane Biol.* **86**, 9—15
- Gray P. T. A., Bevan S., Ritchie J. M. (1984): High conductance anion-selective channels in rat cultured Schwann cells. *Proc. Roy. Soc. London Ser. B.* **221**, 395—409
- Groschner K., Kukovetz W. R. (1992): Voltage-sensitive chloride channels of large conductance in the membrane of pig aortic endothelial cells. *Pflügers Arch.* **421**, 209—217
- Hamill O., Marty A., Neher E., Sakmann B., Sigworth F. J. (1981): Improved patch-clamp techniques for high-resolution current recorded from cells and cell-free membrane patches. *Pflügers Arch.* **391**, 85—100
- Harris A. L., Spray D. C., Bennett M. V. L. (1981): Kinetic properties of a voltage-dependent junctional conductance. *J. Gen. Physiol.* **77**, 95—117
- Hille B. (1992): *Ionic Channels of Excitable Membranes*. Second edition. Sinauer Associates, Inc., Sunderland, Mass., USA
- Hurňák O., Zachar J. (1992): Maxi-chloride channels in L6 myoblasts. *Gen. Physiol. Biophys.* **11**, 389—400
- Hurňák O., Zachar J. (1993): High-conductance chloride channels in BC3H1 myoblasts. *Gen. Physiol. Biophys.* **12**, 171—182
- Jap B. K., Walian P. J. (1990): Biophysics of the structure and function of porins. *Quart. Rev. Biophys.* **23**, 367—403
- Kemp P. J., MacGregor G. G., Olver R. E. (1993): G protein-regulated large-conductance chloride channels in freshly isolated fetal type II alveolar epithelial cells. *Amer. J. Physiol.* **265**, L323—L329
- Krouse M. E., Schneider G. T., Gage P. W. (1986): A large anion-selective channel has seven conductance levels. *Nature* **319**, 58—60
- Läuger P. (1985): Ion channels with conformational substates. *Biophys. J.* **47**, 581—591
- McGill J. M., Basavappa S., Fitz J. G. (1992): Characterization of high-conductance channels in rat bile duct epithelial cells. *Amer. J. Physiol.* **262**, G703—G710
- Millhauser G. L. (1990): Reptation theory of ion channel gating. *Biophys. J.* **57**, 857—864
- Neher E. (1992): Correction for liquid junction potentials in patch clamp experiments; In: *Methods in Enzymology*, vol. 207, pp. 123—131, Academic Press, Inc., New York
- Nelson D. J., Tang J. M., Palmer L. G. (1984): Single-channel recordings of apical membrane chloride conductance in A6 epithelial cells. *J. Membrane Biol.* **80**, 81—89
- Olesen S. P., Bundgaard M. (1992): Chloride-selective channels of large conductance in bovine aortic endothelial cells. *Acta Physiol. Scand.* **144**, 191—198
- Pahapill P. A., Schlichter L. C. (1992): Cl-channels in intact human lymphocytes-T. *J. Membrane Biol.* **125**, 171—183
- Sachs H. G., Stambrook P. J., Ebert J. D. (1974): Changes in membrane potential during the cell cycle. *Exp. Cell Res.* **83**, 362—366

- Schlichter L C , Grygorczyk R , Pahapill P A , Grygorczyk C (1990) A large multiple conductance Cl channel in normal human T lymphocytes *Pflugers Arch* **416**, 413—421
- Schwarze W , Kolb H A (1984) Voltage-dependent kinetic of an anionic channel of large unit conductance in macrophages and myotube membranes *Pflugers Arch* **402**, 281—291
- Stavrovsky I , Hurňák O , Zachar J (1992) Semi-automatic analysis of unit channel conductance from voltage ramp transients *Gen Physiol Biophys* **11**, 401—410
- Takahashi A , Yamaguchi H , Miyamoto H (1993) Change in K⁺ current of HeLa cells with progression of the cell cycle studied by patch-clamp technique *Amer J Physiol* **265**, C328—C336
- Thinnes F P (1992) Evidence for extra-mitochondrial localization of the VDAC/porin channel in eukaryotic cells *J Bioenerg Biomembrane* **24**, 71—75
- Unwin N (1989) The structure of ion channels in membranes of excitable cells *Neuron* **3**, 665—676
- Wang H-Z , Li J , Lemanski L F , Veenstra R D (1992) Gating of mammalian cardiac gap junction channels by transjunctional voltage *Biophys J* **63**, 139—151
- Woll K H , Leibowitz M D , Neumcke B , Hille B (1987) A high-conductance anion channel in adult amphibian skeletal muscle *Pflugers Arch* **410**, 632—640
- Woll K H , Neumcke B (1987) Conductance properties and voltage dependence of an anion channel in amphibian skeletal muscle *Pflugers Arch* **410**, 641—647
- Yaffe D (1968) Retention of differentiation potentialities during prolonged cultivation of myogenic cells *Proc Nat Acad Sci USA* **61**, 477—483
- Zachar J , Hurňák O (1994) Arachidonic acid blocks large-conductance chloride channels in L6 myoblasts *Gen Physiol Biophys* **13**, 193—214

Final version accepted May 10, 1994